Non-Resonant and Resonant X-Ray Scattering Studies on Multiferroic $TbMn_2O_5$

J. Koo,[1] C. Song,[1] S. Ji,[1] J.-S. Lee,[1] J. Park,[1] T.-H. Jang,[1] C.-H. Yang,[1] J.-H. Park,[1,2] Y. H. Jeong,[1] K.-B. Lee,[1,2,*] T. Y. Koo,[2] Y. J. Park,[2] J.-Y. Kim,[2] D. Wermeille,[3,†] A. I. Goldman,[3] G. Srajer,[4] S. Park,[5] and S.-W. Cheong[5,6]

[1]eSSC and Department of Physics, POSTECH, Pohang 790-784, Korea
[2]Pohang Accelerator Laboratory, POSTECH, Pohang 790-784, Korea
[3]Ames Laboratory, Department of Physics and Astronomy, Iowa State University, Ames, Iowa 50011, USA
[4]Advanced Photon Source, Argonne National Laboratory, Argonne, Illinois 60439, USA
[5]Rutgers Center for Emergent Materials and Department of Physics and Astronomy, Rutgers University, Piscataway, New Jersey 08854, USA
[6]Laboratory of Pohang Emergent Materials and Department of Physics, POSTECH, Pohang 790-784, Korea

(Received 18 February 2007; published 8 November 2007)

Comprehensive x-ray scattering studies, including resonant scattering at Mn L, Tb L, and M edges, were performed on single crystals of $TbMn_2O_5$ for crystallographic data to elucidate the nature of its commensurate and incommensurate phases. The scattering results provide direct evidence of symmetry lowering to the ferroelectric phase driven by magnetically induced lattice modulations and show the presence of multiple magnetic orders. The competing orders under spin-frustrated geometry are believed to cause discommensuration and result in the commensurate-to-incommensurate phase transition around 24 K. It is proposed that the low temperature incommensurate phase consists of commensurate domains separated by antiphase domain walls which change both signs of spontaneous polarizations and x-ray scattering amplitudes for forbidden reflections.

DOI: 10.1103/PhysRevLett.99.197601 PACS numbers: 77.80.−e, 61.10.−i, 64.70.Rh, 75.25.+z

In recent years, multiferroic materials, in which magnetic and ferroelectric orders coexist and are cross-correlated [1–10] have attracted much attention due to theoretical interests and potential magnetoelectric (ME) device applications. Manipulation of electric polarizations by external magnetic fields has been demonstrated in some of these materials [4,5]. Orthorhombic $TbMn_2O_5$, one of the multiferroic materials, displays a rich phase diagram. Upon cooling through $T_N \sim 41$ K, $TbMn_2O_5$ becomes antiferromagnetic with an incommensurate magnetic (ICM) order which transits to a commensurate magnetic (CM) phase with spontaneous electric polarization at $Tc1 \sim 36$ K, and reenters a low temperature incommensurate magnetic (LT-ICM) phase at $T_{c2} \sim 24$ K. Anomalies of ferroelectricity and dielectric properties were observed concurrently with these magnetic phase transitions [4,9]. Especially, the reentrant LT-ICM phase is a phenomenon peculiar to $R$$Mn_2O_5$ multiferroics while commensurate phases are more common as the low temperature ground states. Since the CM to LT-ICM phase transition is also accompanied with an abrupt loss of spontaneous polarizations, it is critical to elucidate the natures of the incommensurability of the material, including the mechanism of the CM to LT-ICM phase transition.

The origin of the complex phases of the material is attributed to the coupling between magnetic moments of Mn ions and lattice [8,9]. It is suggested that when a magnetic order is modulated with a propagation vector $\boldsymbol{q}_m$, the exchange striction results in a periodic lattice modulation with a propagation vector $\boldsymbol{q}_c = 2\boldsymbol{q}_m$ [5–9]. Recently, Chapon *et al.* proposed for $R$$Mn_2O_5$ systems that ferroelectricity results from acentric spin-density waves for the CM phases [9]. Indeed, Kimura *et al.* insisted that CM modulations are indispensable to the ferroelectricity in the LT-ICM phase, from their neutron scattering results on $HoMn_2O_5$ under high magnetic fields [11]. Betouras *et al.* recently proposed a model for multiferroicity induced by dislocated spin-density waves. According to the model, the commensurability is crucial for the onset of ferroelectricity [12]. However, spontaneous polarizations are observed in the LT-ICM phases and lattice distortions derived from ICM spin structures turned out to describe well the polarizations of YMn_2O_5 even in the phase [13], implying that commensurability is not a necessary condition for the ferroelectricity. In order to understand the intriguing ME well, detailed information on the lattice and spin structure changes is necessary. However, only limited crystallographic data are available, and even any direct evidence on the symmetry lowering has not been reported yet [9–11,13–15].

In this Letter, we present synchrotron x-ray scattering results on single crystals of $TbMn_2O_5$. A (3 0 0) forbidden Bragg peak, which is a direct evidence of the symmetry lowering to a noncentrosymmetry space group, was observed in the ferroelectric (FE) phases. Furthermore, the temperature dependence of the peak intensity, $I_{(300)}$, was found to coincide with those of the lattice modulation peak intensities, I_c, and the spontaneous polarization square, P^2, in the CM phase. This indicates the ferroelectricity is generated by the lattice modulations. In the LT-ICM phase, temperature dependences of I_c cannot be described by a single order parameter, implying the presence of different magnetic orders. Resonant x-ray magnetic scattering results at Mn L, Tb L_3, and M_5 edges show that each magnetic order has its own temperature dependence. It is proposed that CM to LT-ICM phase transition is induced by discommensuration through phase slipping due to competing magnetic orders under the frustrated geometry. Moreover, the CM modulations with antiphase domain walls are consistent with the temperature dependences of $\boldsymbol{q}_m$ in the LT-ICM phase, and explain well the abrupt loss of P and $I_{(300)}$ at the transition.

Single crystals of $TbMn_2O_5$ were grown by a flux method [4]. The specimen used for the hard x-ray scattering measurements has a platelike shape with [1 1 0] as a surface normal direction. Its mosaicity was measured to be about 0.01° at (3 3 0) Bragg reflection. For soft x-ray scattering, a different sample was cut and polished to have [2 0 1] as a surface normal direction. Soft x-ray scattering measurements were performed at the 2A beam line in the Pohang Light Source (PLS). Details of the soft x-ray scattering chamber were described elsewhere [16]. X-ray diffraction experiments were conducted at the 3C2 bending magnet beam line in the PLS and at the 6-ID undulator beam line in the Midwest Universities Collaborative Access Team (MUCAT) Sector in the Advanced Photon Source. For nonresonant x-ray scattering experiments, 6.45 keV was selected as an incident x-ray energy below Mn K edge (~6.55 keV). All the incident x-rays were σ-polarized, and PG(006) was used to have a σ-to-π channel at Tb L_3 edge.

Nonresonant x-ray scattering measurements were performed. Results of simultaneous measurements of $\boldsymbol{q}_m$ and $\boldsymbol{q}_c$, not shown here, show similar temperature dependence of $\boldsymbol{q}_m$ reported from neutron scattering results of others [17], and confirm the relationship of $\boldsymbol{q}_c = 2\boldsymbol{q}_m$. As shown in Fig. 1(a), measurable x-ray intensities were observed, in the FE phase, at (3 0 0) Bragg position which is forbidden under a space group of the room temperature paraelectric phase, Pbam. Residual intensities above T_{c1} are due to higher harmonic contaminations. Values for full-width-at-half-maximum of the peak are about 0.01°, close to those of (4 0 0) main Bragg peak in the LT-ICM phase. The results explicitly evidenced that inversion symmetry is broken concomitantly with the FE phase as speculated before [9,10]. According to the models, displacements of Mn^{3+} are in ab-plane. While b-axis components of the atomic displacements mainly contribute to P, a-axis components enable the emergence of $I_{(300)}$. If the atomic displacements correspond to the periodic lattice modulations, it is expected that both P^2 and $I_{(300)}$ are proportional to I_c, which is consistent with experimental results shown in Fig. 1(b). (The data of P^2 are taken from Ref. [4] and are shifted in order to get the same values for T_{c1}.) This confirms that spontaneous polarization is due to the atomic displacements driven by magnetic orders: a direct crystallographic evidence for the origin of ferroelectricity in the material [8–10,13].

Though many interesting ME phenomena have been reported in the LT-ICM phases below T_{c2} [4,11,18,19], their basic mechanisms still remain to be understood. Since the lattice modulations reflect basic ME natures, temperature dependences below T_{c2} of integrated intensities were measured at the four split ICM peak positions illustrated in Fig. 2(a). From the results displayed in Fig. 2(b), it is clear that temperature dependences of all four peaks cannot be described by a single order parameter, implying the presence of various magnetic orders having the same $\boldsymbol{q}_m$'s but different temperature dependences. The result is consistent with our recent neutron scattering measurements for temperature dependences of magnetic satellite intensities [20].

To confirm the presence of multiple magnetic orders, we performed resonant x-ray magnetic scattering measurements at Mn L, Tb L_3, and M_5 edges. Figure 3(a) shows energy profiles around Mn L edge of magnetic satellites at 10 K and x-ray absorption spectroscopy (XAS) at room temperature. Magnetic peaks and XAS data clearly show

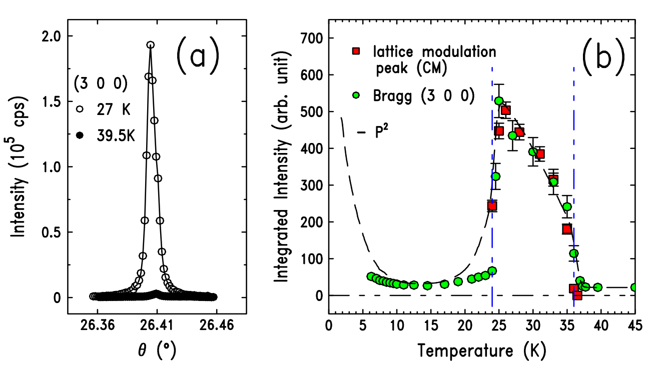

FIG. 1 (color online). (a) Rocking curves of a (3 0 0) forbidden Bragg peak measured below (open line) and above T_{c1} (solid line). (b) Temperature dependences of the integrated intensities of a (3 0 0) Bragg peak (circle), CM lattice modulation peak (square), and squared spontaneous polarization (broken line) taken from Ref. [4]. All the data are properly scaled.

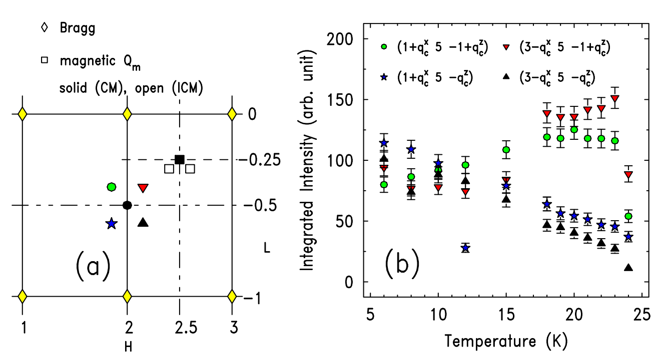

FIG. 2 (color online). (a) Positions of measured magnetic satellites (square) and lattice modulation peaks in the (h 5 l) reciprocal lattice plane (circles, triangles, and star). The solid circle represents a CM lattice modulation peak position. (b) Temperature dependences of the ICM lattice modulation peak intensities.

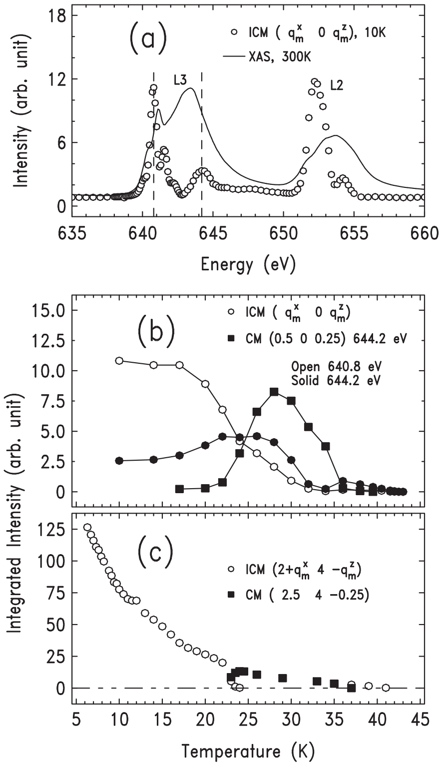

FIG. 3. (a) Energy profiles of the ICM magnetic peaks (circle)and XAS (solid line) around Mn L edges. Vertical broken lines correspond to 640.8 and 644.2 eV, respectively. (b) Temperature dependences of the ICM (circle) and the CM (square) magnetic peaks. Open (solid) symbols denote the data taken $E = 640.8$ eV (644.2 eV), respectively. (c) Temperature dependences of the ICM (open circle) and the CM (solid square) magnetic peak at Tb L_3 edge.

resonances at both Mn L_2 and L_3 edges. XAS results show broad peaks containing contributions from the multiplet states of $3d$ electrons of Mn^{3+} and Mn^{4+} ions. Magnetic satellites show relatively sharp double peaks at both Mn L edges. The sharp resonances represent different multiplet states of Mn $3d$ electrons including charge transfer excitations, while Mn ions are expected to be in the high-spin configurations with all the $3d$ electron spins aligned parallel. Therefore, although the resonances do not have one-to-one correspondences with the magnetic orders of Mn ions, changes in the resonances at magnetic satellites reflect the changes in spin ordering which are periodically modulated with the propagation vector $\boldsymbol{q}_m$. Temperature dependences of x-ray intensities at the ICM peak of $\boldsymbol{Q}_m = (q_m^x\ 0\ q_m^z)$ were measured at the two resonances, 640.8 and 644.2 eV. The energy of 640.8 eV is close to that of the characteristic state of Mn^{2+} ions located at surfaces as suggested for $La_{0.7}Sr_{0.3}MnO_3$ thin films [21]. However, the peak in our measurement is a well-ordered three-dimensional peak having a correlation length of 500 Å along the surface normal direction, excluding any possibility of the peak from surface states. Their temperature dependences are presented in Fig. 3(b). Data for a CM peak of $\boldsymbol{Q}_m = (0.5\ 0\ 0.25)$ at the resonance of 644.2 eV are presented together. It is clear that, above 15 K, intensities of each resonance have different temperature dependences from each other. Though the origin of the anomalous temperature dependences is not understood in detail, it reflects complicated natures of magnetic moments of Mn ions under the frustrated configuration and the presence of multiple magnetic orders on Mn ions.

Magnetic ordering of Tb^{3+} ions was investigated with resonant x-ray scattering measurements at Tb L_3 edge. Figure 3(c) shows that ordering temperature of Tb magnetic moments is the same with that of Mn, T_N, which is consistent with neutron scattering results [9]. The resonant magnetic x-ray scattering intensities were measured at the same magnetic satellite peak in nonresonant x-ray scattering measurements. Soft x-ray magnetic scattering measurements were also performed at Tb M_5 edge, and the result, not shown here, confirms that observed x-ray intensities in Fig. 3(c) reflect magnetic order of Tb $4f$ electrons which grows monotonically below T_N.

From the results in Fig. 3(b) and 3(c), it is clear that there exist multiple magnetic order parameters having the same $\boldsymbol{q}_m$'s but different temperature dependences. The contributing portions of each magnetic order to scattering factors for magnetic satellites are different depending on $\boldsymbol{Q}_m (= \boldsymbol{Q}_{\mathrm{Bragg}} + \boldsymbol{q}_m)$, and it results in different temperature dependence for each magnetic peak and its corresponding lattice modulation peak intensities, which explains the temperature dependences presented in Fig. 2(b).

Since the magnetic orders are located under the spin-frustrated geometry, it is reasonable to suppose that phase-slips take place due to competitions between the magnetic orders, as their order parameters change with different temperature dependences as shown in Fig. 3(b) and 3(c). The discommensuration results in the transition to the LT-ICM phase. An antiphase domain wall is a natural choice of the phase slip since the two domains have the equal energy minima. For spin-density waves with a propagation vector of (0.5 0 0.25), a phase-shift by π is equivalent to a translation by one unitcell along a-direction. Assuming the antiphase domain wall causes a shift of π in relative phase between spin modulations of the adjacent a-direction Mn-O chains in ab-plane, canted antiferroelectric displacements of Mn^{3+} ions in the plane [9] reverse their directions as shown schematically in Fig. 4. The left and right panels of Fig. 4 show the displacements of Mn^{3+} ions in unitcells across an antiphase domain wall. Although there also exist displacements of other ions, our argument here is about the symmetry and can be generalized to take account of them. Across the domain wall, directions of the atomic displacements and the spontaneous polarizations are reversed. Only a-components of the displacements are relevant to x-ray structure factors for (h = odd 0 0) reflections. As far as the a-components are concerned, two unitcells across the domain wall would be identical if one of them is translated by halfway along the a-direction. Therefore, structure factors

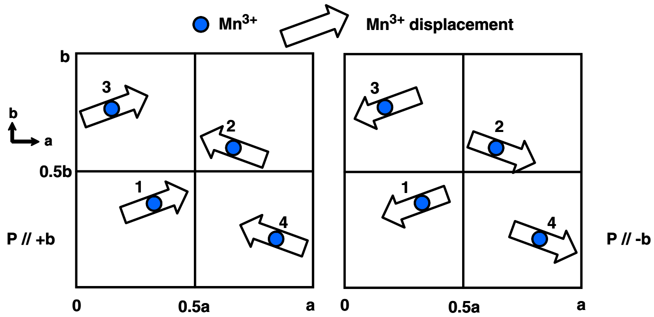

FIG. 4 (color online). A schematic drawing of lattice displacements of Mn^{3+} ions in unitcells across an antiphase domain wall.

of the two unitcells for (h = odd 0 0) reflections are different by a factor of $e^{i\pi}$ ($=-1$) from each other. Not only do the polarizations of domains separated by the domain wall cancel each other but also their x-ray scattering amplitudes for (3 0 0) Bragg peak do the same because of the crystal symmetry. Then, only remnants due to unequal domain populations contribute to P and $I_{(300)}$, which explains their abrupt decreases at T_{c2}. The above discussions are mainly about contributions from Mn-O networks. Therefore, it is applicable to the generic behavior of CM to LT-ICM phase transitions in RMn$_2$O$_5$ family.

Tb magnetic moments also couple with lattices [18,19,22], and their effects get larger at lower temperature [22] due to their enhanced magnitudes shown in Fig. 3(c). Discrepancy between temperature dependences of P and $I_{(300)}$ in Fig. 1(b) is attributed to lattice modulations induced by enhanced Tb magnetic moments in the LT-ICM phase. It is well known that R^{3+} ions of RMn$_2$O$_5$ family play important roles in their ME phenomena at low temperature [11,15]. Therefore, sizable effects of Tb moments are anticipated in the LT-ICM phase, and details of the effects on lattices need further studies.

Since a density of the domain walls determines $\boldsymbol{q}_m$, the temperature dependence of $\boldsymbol{q}_m$ can be also explained consistently in terms of CM modulations with the antiphase domain walls. This indicates that CM modulations are preferred as its low temperature ground state. Then, the low temperature phase seems to have a higher entropy due to the domain walls than the high temperature CM phase, violating the entropy rule. However, due to the geometrical frustration and the presence of multiple magnetic orders, many different energy scales can exist. The complicated temperature dependences of Mn magnetic orders in Fig. 3(b) reflect the presence of the different energy scales. Smaller energy scales become important at low temperatures and induce discommensuration.

In summary, we have confirmed from crystallographic data that ferroelectricity of TbMn$_2$O$_5$ is indeed driven by magnetically induced lattice modulation. It was demonstrated by the same temperature dependences of P^2, $I_{(300)}$, and I_c in the CM FE phase. The presence of multiple magnetic orders was demonstrated by different temperature dependences of resonant magnetic x-ray scattering intensities. The CM to LT-ICM phase transition is attributed to discommensuration due to competing magnetic orders of Mn ions in the frustrated configurations. Temperature dependences of $\boldsymbol{q}_m$ and $I_{(300)}$ in the LT-ICM phase can be explained in terms of the CM modulations with antiphase domain walls, while contributions from enhanced Tb magnetic moments become important at low temperature.

We thank D. J. Huang for the useful discussions. This work was supported by the KOSEF through the eSSC at POSTECH, and by MOHRE through BK-21 program. The experiments at the PLS were supported by the POSTECH Priority Research program and MOST. The work at the Advanced Photon Source was supported by the U.S. DOE, Office of Science, Contract No. DE-AC02-06CH11357. The Midwest Universities Collaborative Access Team (MUCAT) sector at the APS is supported by the U.S. Department of Energy, Office of Science, Office of Basic Energy Sciences, through the Ames Laboratory under Contract No. DE-AC02-07CH11358. Work at Rutgers was supported by No. NSF-DMR-0520471.

*kibong@postech.ac.kr
†Present address: European Synchrotron Radiation Facility, BP 220, F-38043 Grenoble Cedex 9, France.

[1] M. Kenzelmann *et al.*, Phys. Rev. Lett. **95**, 087206 (2005).
[2] G. Lawes *et al.*, Phys. Rev. Lett. **95**, 087205 (2005).
[3] S. Kobayashi *et al.*, J. Korean Phys. Soc. **46**, 289 (2005).
[4] N. Hur *et al.*, Nature (London) **429**, 392 (2004).
[5] T. Kimura *et al.*, Nature (London) **426**, 55 (2003).
[6] T. Goto *et al.*, Phys. Rev. Lett. **92**, 257201 (2004).
[7] T. Kimura *et al.*, Phys. Rev. B **68**, 060403(R) (2003).
[8] S.-W. Cheong *et al.*, Nat. Mater. **6**, 13 (2007).
[9] L. C. Chapon *et al.*, Phys. Rev. Lett. **93**, 177402 (2004).G. R. Blake *et al.*, Phys. Rev. B **71**, 214402 (2005).
[10] I. Kagomiya *et al.*, Ferroelectrics **286**, 167 (2003).
[11] H. Kimura *et al.*, J. Phys. Soc. Jpn. **75**, 113701 (2006).
[12] J. J. Betouras *et al.*, Phys. Rev. Lett. **98**, 257602 (2007).
[13] L. C. Chapon *et al.*, Phys. Rev. Lett. **96**, 097601 (2006).
[14] V. Polyakov *et al.*, Physica B (Amsterdam) **297**, 208 (2001).
[15] D. Higashiyama *et al.*, Phys. Rev. B **70**, 174405 (2004).
[16] J.-S. Lee, Ph.D. Thesis, POSTECH, 2006.
[17] S. Kobayashi *et al.*, J. Phys. Soc. Jpn. **73**, 3439 (2004).
[18] S. Y. Haam *et al.*, Ferroelectrics **336**, 153 (2006).
[19] S.-H. Baek *et al.*, Phys. Rev. B **74**, 140410(R) (2006).
[20] J. Koo *et al.*, J. Korean Phys. Soc. **51**, 562 (2007).
[21] M. P. de Jong *et al.*, Phys. Rev. B **71**, 014434 (2005).
[22] R. Valdés Aguilar *et al.*, Phys. Rev. B **74**, 184404 (2006).